



# Monitoring of waste rock dump surface water drainage and channel infiltration

Jason Keller<sup>1</sup>, Jaime Banuelos<sup>2</sup>, Lindsey Bunting<sup>2</sup>, Mike Milczarek<sup>2</sup>, Robert Rice<sup>2</sup>, Daniel Lattin<sup>3</sup>,

<sup>1</sup>*GeoSystems Analysis, Inc., Hood River, OR, USA*

<sup>2</sup>*GeoSystems Analysis, Inc., Tucson, AZ, USA*

<sup>3</sup>*Homestake Mining Company, Lower Lake, CA, USA*

<sup>4</sup>*Barrick Gold Corporation, Salt Lake City, UT, USA*

## Abstract

A series of low-cost, high-resolution game cameras (flow-imagery) and resistance sensors (inundation sensors) were installed in unlined drainage channels at a reclaimed waste rock dump (WRD) to determine the distribution, duration and estimated infiltration of surface water into the channel areas. Estimated drainage channel infiltration from the flow-imagery and inundation sensor data was 3.6 percent of the estimated WRD seepage collection volume during the same monitoring time period. The flow-imagery and inundation sensor monitoring results provided a clear indication that most of the water entering the WRD seepage collection pond is from a source other than drainage channel infiltration.

**Keywords:** Infiltration, Seepage, Flow-imagery, Inundation, Monitoring

## Introduction

Surface water flow over unlined drainage channels can be a primary source of net infiltration into closed waste rock dump (WRD) facilities in semi-arid regions (Flint and Flint, 2007; Scanlon et al., 1999; Zhan et al., 2014). Thus, understanding the contribution of net infiltration into unlined drainage channels to a WRD water budget is important to prioritize closure design efforts to minimize seepage from closed WRD facilities.

A relatively inexpensive and efficient method to quantify drainage channel flow characteristics and infiltration is the use of low-cost, high-resolution game cameras to monitor surface water depth and event duration (flow-imagery). Low cost resistance sensors can also be installed to detect the onset and duration of surface inundation (the beginning and end of a flow event) and provide a high-resolution complement to flow-imagery.

To determine the distribution, duration and estimated infiltration of surface water in unlined drainage channel areas, a series of game cameras and inundation sensors were installed at different locations at a closed and

reclaimed WRD. The site is located in a temperate Mediterranean climate that receives approximately 800 mm/yr of precipitation, which mostly occurs between the months of December to March. Annual average minimum and maximum temperature is 8 °C and 22 °C, respectively.

## Methods

In February 2015, five inundation monitoring stations were installed along western and southern portions of a bench on a closed WRD. Stations were located in areas known to collect and pond surface water runoff. Three stations were located on the western portion of the WRD bench (W1, W2, W3) and two stations on the southern portion of the bench (S1 and S2). Each station included one game camera, two staff gauges to estimate the water ponding depth from the flow-imagery, and four resistance sensors equally spaced across the monitoring area. The total length of each monitoring location ranged from 49 m to 100 m.

Game cameras (Reconyx Hyperfire, WI, USA) were fastened to t-posts and programmed to take a photograph every fifteen minutes (Figure 1). Two staff gages were in-



stalled at each location; one at 4.6 m and a second at 9.1 m from the camera. Reflective tape was placed across the gages at 15 cm intervals to provide added visibility for images taken at night. Pin flags were placed at 1.5 m intervals laterally from each staff gage, perpendicular to the field of view and towards the channel edges to allow for visual estimation of lateral water extent during inundation events.

Resistance sensors (GSA, AZ, USA) were installed at the low point in the drainage channels and connected to an EM50 datalogger (Decagon, WA, USA). These sensors function by measuring the resistance between two stainless steel probes exposed above the soil surface (Figure 1). Dataloggers were pro-

grammed to record sensor readings every five minutes.

## Results

The study period extended from March 1, 2015 to March 31, 2016. Mine site monthly precipitation rates for the monitoring period, along with historical mean monthly precipitation, are presented in Figure 2. Total precipitation for the monitoring record was 56.9 cm, compared to a historic mean of 77.2 cm for the same 13-month period. Precipitation during the study period generally followed historic precipitation trends, however, cumulative annual precipitation at the beginning of the monitoring period (late winter, 2015)



**Figure 1** A) Inundation sensor, B) camera installed on t-post for flow-imagery monitoring, C) sample flow-imagery image, including flagging.



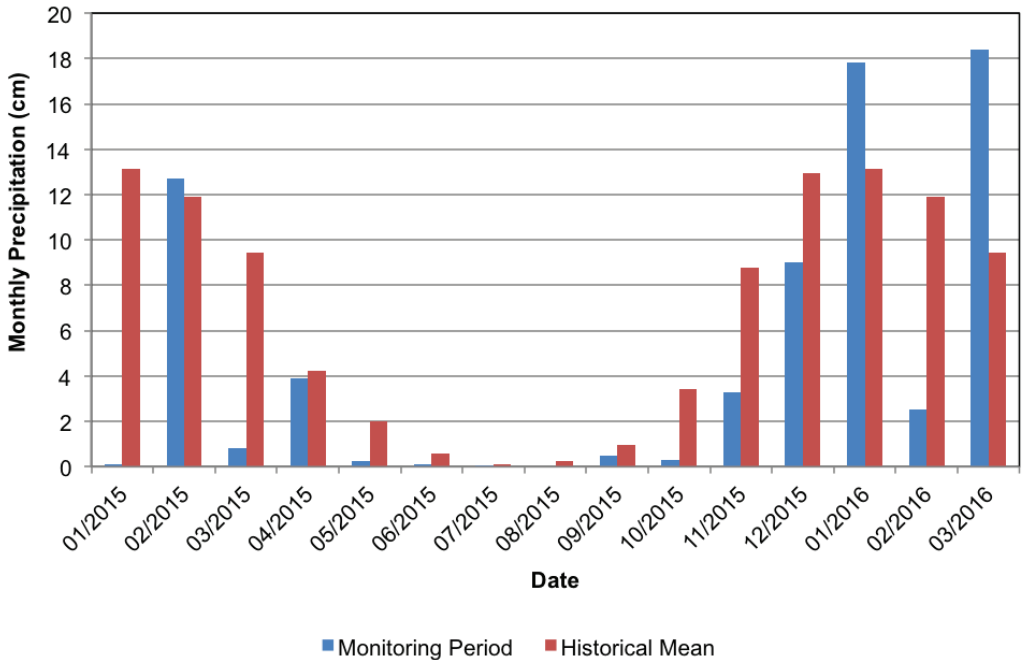


Figure 2 Mean monthly precipitation for the monitoring period and historical average (November 1954 to March 2016)

was far below average with a total precipitation of 13.6 cm compared to a historic mean of 34.5 cm. A precipitation total of 47.7 cm was measured from December 2015 through March 2016, approximately equal to the historic precipitation average of 47.4 cm for this four-month period.

Flow-imagery photos over each inundation event were analyzed to determine the hourly inundation area and depth of inundation within the field of view of the camera. Resistance sensor response was then analyzed to estimate the inundation area length, total inundation area, and inundation start and end times. The width of the inundation area observed in the photo was assumed to exist over the entire length of the inundation area.

Figure 3 presents an example of a flow-image during an inundation event at the S1 monitoring location and the change in water depth from the start to the end of inundation. Over the monitoring period, observed inundation water levels were generally below 15 cm, with the highest water level observed being 41 cm.

Resistance sensors recorded less than -50 ohms under dry conditions (no inundation)

and greater than -50 ohms when inundated with water. Figure 4A shows an example of an inundation event at the S1 monitoring location as indicated by a sharp decrease in resistance for the duration of inundation; Figure 4B presents an example of the estimated inundation area over the same time period. The inundation area was observed to increase with increasing precipitation. After precipitation stopped, individual inundation sensors responded depending on location. Sensors S1-1 and S1-4 were furthest from the center of the inundation area and were first to record less than -50 ohms as the precipitation event ceased and the inundation area decreased. The two middle sensors (S1-2 and S1-3) measured inundation for longer.

Inundation periods were observed between December 2015 and March 2016, coinciding with the months of increased precipitation. Inundation duration ranged from 2 hours to 645 hours and a maximum wetted area over all five stations of approximately 1,170 m<sup>2</sup> was observed.

Flow-imagery photos were analyzed for each inundation event to determine the rate of change in water depth to estimate the infil-







Figure 3 Inundation event from March 10, 2016 08:00 to March 17, 2016 09:00

tration rates of for each area. Infiltration rates were calculated by dividing the change in water depth by the duration of infiltration. Table 1 presents the geometric mean calculated infiltration rates for each station. Geometric mean infiltration rates calculated from the inundation events ranged from  $6.8 \times 10^{-6}$  cm/sec to  $7.7 \times 10^{-5}$  cm/sec.

Hourly infiltration volumes resulting from each inundation event at each station were calculated by multiplying the infiltration rate by the estimated hourly inundation area. Hourly infiltration volumes were then summed over each inundation event to estimate the total volume of infiltration. Table 2 presents the monthly total estimated infiltration volumes for each station and for all monitoring stations combined. The total estimated infiltrated volume over the period of monitoring was  $396 \text{ m}^3$ . Dividing the estimated infiltrated volume by the total drainage channel monitored area ( $1,407 \text{ m}^2$ ), equates to  $0.3 \text{ m}^3$  of infiltration per  $1 \text{ m}^2$ .

To estimate the infiltration volumes for all drainage channels on the WRD, the monthly

infiltration volume per area of drainage channel (Table 2) was multiplied by the estimated drainage channel area on all WRD benches. The actual area that inundates on other drainage channel areas was not known but was assumed to be 25 percent of the total drainage channel area based on the area known to become inundated within the monitored drainage channel area.

Estimated total WRD infiltration volumes are presented in Table 3. The total estimated WRD drainage channel infiltration volume for the monitoring period was  $2,200 \text{ m}^3$ . Estimated drainage channel infiltration volumes were compared to actual WRD seepage collection volumes for the time period of December 2015 to March 2016. WRD seepage collection volumes follow monthly precipitation and infiltration trends, and, therefore, monthly seepage collection volumes were assumed to include drainage channel infiltration volumes for similar months (i.e. no time lag). Through December 2015 through March 2016, the total estimated WRD drainage channel infiltration volume ranged from



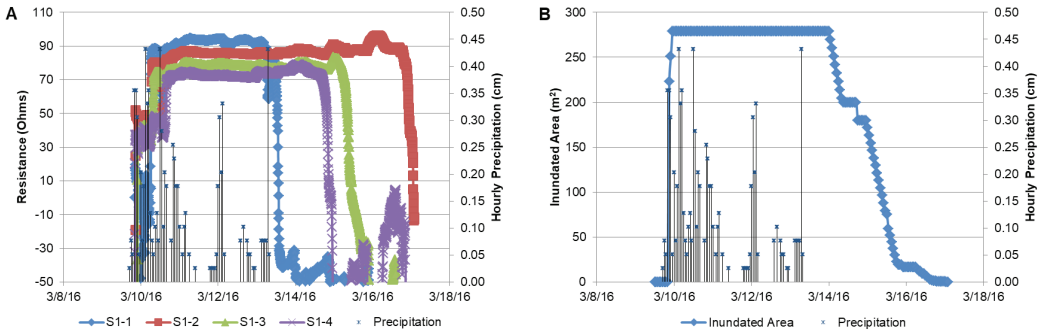


Figure 4 A) Measured resistance and precipitation, and B) estimated inundated area and precipitation from March 10, 2016 08:00 to March 17, 2016 09:00

Table 1. Geometric mean calculated infiltration rate

Station	Geometric Mean Infiltration Rate (cm/s)
W1	1.2E-05
W2	1.1E-05
W3	6.8E-06
S1	7.7E-05
S2	2.5E-05

Table 2. Estimated station infiltration volume

Month	Station					Monthly Total	
	S1	S2	W1	W2	W3	m <sup>3</sup>	(m <sup>3</sup> /m <sup>2</sup> Drainage Channel) <sup>1</sup>
12/2015	0	0	0	0	1	1	0.0
01/2016	78	25	17	32	11	163	0.1
02/2016	0	0	0	0	0	1	0.0
03/2016	117	41	36	22	16	232	0.2
Total	194	67	52	55	28	396	0.3

<sup>1</sup>Total monitoring station surface area: 1,407 m<sup>2</sup>

Table 3. WRD seepage collection volumes and estimated bench drainage channel infiltration volumes

Month	Seepage Collection Volumes		Drainage Channel Infiltration Volumes
	m <sup>3</sup>	m <sup>3</sup>	Percent of Total Seepage Collection Volume
12/2015	9,600	0	0.0
01/2016	14,300	900	6.3
02/2016	11,500	0	0.0
03/2016	26,500	1,300	4.9
Total	61,900	2,200	3.6



less than 0.1 percent to 6.3 percent of the total seepage collection volume and averaged 3.6 percent of the seepage collection volume. Even if 100% of the drainage channel area inundated, only 14.4% of the seepage could be attributed to channel infiltration. These results indicate that most water entering the WRD seepage collection pond is from a source other than drainage channel infiltration.

## Conclusions

Low-cost, high-resolution game cameras to monitor surface water depth and event duration in conjunction with resistance sensors to detect the duration of surface inundation offer a relatively inexpensive and efficient method to quantify surface water flow in ephemeral channels and estimate infiltration. Based on flow-imagery and resistance sensor data, drainage channel infiltration volumes were estimated to be 3.6 percent of the WRD seepage collection volume during the same monitoring time period. These results provide a clear indication that most of the water entering the WRD seepage collection pond is from a source other than drainage channel infiltration.

## Acknowledgements

The authors thank staff and management at Homestake Mining Company and Barrick Gold Corporation for their support of this

project and for permitting the presentation of this work. Special thanks to Homestake Mining Company support staff for maintaining equipment and downloading data.

## References

- Flint AL, Flint LE (2007) Application of the basin characterization model to estimate in-place recharge and runoff potential in the basin and range carbonate-rock aquifer system, White Pine County, Nevada, and adjacent areas in Nevada and Utah. USGS Scientific Investigation Report 2007–5099, Washington DC, USA
- Scanlon BR, Langford RP, Goldsmith RS (1999) Relationship between geomorphic settings and unsaturated flow in an arid setting. *Water Resour Res* 35:983–999
- Zhan G, Keller J, Milczarek M, Giraud J (2014) 11 years of evapotranspiration cover performance at the AA leach pad at Barrick Goldstrike Mines. *Mine Water Environ* 33(3):195-205, doi:10.1007/s10230-014-0268-6

